Optimization of Electrochemical Aptamer-Based Sensors via Optimization of Probe Packing Density and Surface Chemistry

Ryan J. White[†], **Noelle Phares**[†], **Arica A. Lubin**[†], **Yi Xiao**[†], and **Kevin W. Plaxco**[*,†,‡]

[†] *Department of Chemistry and Biochemistry, University of California, Santa Barbara, Santa Barbara, California 93106-9510*

[‡] *Interdepartmental Program in BioMolecular Science and Engineering, University of California, Santa Barbara, Santa Barbara, California 93106-9510*

Abstract

Electrochemical, aptamer-based (E-AB) sensors, which are comprised of an electrode modified with surface immobilized, redox-tagged DNA aptamers, have emerged as a promising new biosensor platform. In order to further improve this technology we have systematically studied the effects of probe (aptamer) packing density, the AC frequency used to interrogate the sensor, and the nature of the self-assembled monolayer (SAM) used to passivate the electrode on the performance of representative E-AB sensors directed against the small molecule cocaine and the protein thrombin. We find that, by controlling the concentration of aptamer employed during sensor fabrication, we can control the density of probe DNA molecules on the electrode surface over an order of magnitude range. Over this range, the gain of the cocaine sensor varies from 60% to 200%, with maximum gain observed near the lowest probe densities. In contrast, over a similar range, the signal change of the thrombin sensor varies from 16% to 42% and optimal signaling is observed at intermediate densities. Above cut-offs at low hertz frequencies, neither sensor displays any significant dependence on the frequency of the alternating potential employed in their interrogation. Finally, we find that E-AB signal gain is sensitive to the nature of the alkanethiol SAM employed to passivate the interrogating electrode; while thinner SAMs lead to higher absolute sensor currents, reducing the length of the SAM from 6-carbons to 2-carbons reduces the observed signal gain of our cocaine sensor 10-fold. We demonstrate that fabrication and operational parameters can be varied to achieve optimal sensor performance and that these can serve as a basic outline for future sensor fabrication.

Introduction

Recent years have seen the emergence of a new class of electrochemical sensors, sometimes termed electrochemical aptamer-based (E-AB) sensors, predicated on the binding-induced folding of DNA or RNA aptamers and directed against targets ranging from proteins[1–5] to small molecules[6–9] to inorganic ions.[10,11] Signal generation in the E-AB platform occurs when target binding alters the folding and flexibility of an electrode-bound aptamer (Figure 1). This, in turn, results in a readily measurable change in faradaic current from an attached redox tag. Because the sensing aptamer, and its attached redox tag, are strongly bonded to the interrogating electrode, E-AB sensors are reagentless and readily reusable.[3,6] Likewise, because E-AB signaling is linked to a binding-specific change in the folding and dynamics of the sensing aptamer (and not simply a response to the adsorption of mass or charge to the sensor surface),[12] E-AB sensors are relatively insensitive to the nonspecific binding of interferants and perform well even when challenged directly in blood serum and other complex sample

---

* To whom correspondence should be addressed. E-mail: E-mail: kwp@chem.ucsb.edu.

matrices.[3,6] Given these attributes, the E-AB platform appears a promising and potentially general biosensor approach.[13,14]

Despite the relatively large number of E-AB sensors reported to date[1–11] few, if any, systematic studies have yet examined the extent to which varying E-AB fabrication and/or operational parameters impact sensor performance. For example, because E-AB signaling likely arises due to a binding-induced change in collision dynamics between the redox tag and the electrode surface,[15] molecular crowding (as measured by the density of aptamer probes on the electrode surface) may effect both sensor gain and equilibration time (see by analogy refs 15–17). Similarly, because E-AB signaling arises due to changes in electron transfer dynamics, the frequency of the AC current used to interrogate the sensor and the nature of the self-assembled monolayer (SAM) through which the electrons must transfer likely also affect sensor performance. Here we investigate the effects of these parameters on signal gain, equilibration time, and binding affinity for two representative E-AB sensors.

Materials and Methods

Reagents and DNA Probes

Cocaine, 6-mercapto-1-hexanol (C6), 3-mercapto-1-propanol (C3), 2-mercaptoethanol (C2), Trizma preset crystals at pH 7.4, and sulfuric acid (Sigma Aldrich) were used as received. Hexaammineruthenium(III) chloride (RuHex; Strem Chemicals Inc., Newburyport, MA) was used as received. Human α-thrombin (Haematologic Technologies Inc.; Essex Junction, VT) was diluted in Tris buffer (0.1 M Tris pH 7.4 with 140 mM NaCl, 20 mM $MgCl_2$, and 20 mM KCl) to a final, sensor saturating concentration of 750 nM. This buffer was employed in all thrombin sensor experiments. For all cocaine sensor experiments, a 20× saline-sodium citrate buffer (SSC; Sigma Aldrich) was diluted 20-fold prior to use with ultrapure water (18 MΩ·cm Milli-Q Ultrapure Water Purification, Millipore, Billerica, MA) to yield a 150 mM NaCl, 15 mM sodium citrate buffer (pH 7.0) buffered solution. The 5′-thiol-, 3′-methylene blue-modified DNA aptamer sequences (HPLC-purified, Biosearch Technologies, Inc. Novato, CA) were used as received without further purification. The cocaine sensor sequence employed was 5′-HS-$(CH_2)_6$-AGA CAA GGA AAA TCC TTC AAT GAA GTG GGT CG-$(CH_2)_7$-methylene blue-3′, and the thrombin sensor sequence was 5′-HS-$(CH_2)_6$-TAA GTT CAT CTC CCC GGT TGG TGT GGT TGG T-$(CH_2)_7$-methylene blue-3′, both as previously reported.[3,6]

Sensor Fabrication

A detailed description of E-AB sensor fabrication may be found in the literature.[18] In brief, E-AB sensors were fabricated on gold rod electrodes (1.6 mm diameter, BAS, West Lafayette, IN). Prior to modification the electrodes were polished with a 1 μm diamond suspension in oil (Buehler, Lake Bluff, Il) followed by a 5 min sonication in ethanol. The electrodes were further polished using 0.5 μm alumina oxide particles (Buehler) suspended in water. This step was followed by sonication in water for 5 min. A series of oxidation and reduction cycles in 0.5 M H_2SO_4, 0.01 M KCl/0.1 M H_2SO_4, and 0.05 M H_2SO_4 were performed in order to further clean the electrodes. Electrode area was determined from the gold oxide reduction peak obtained in the 0.05 M H_2SO_4 solution. Following this cleaning, the electrode was modified with the probe aptamer as follows. A stock solution of the aptamer (0.2 mM) was first reduced in 1 μM tris (2-carboxyethyl) phosphine hydrochloride for 1 h to cleave any disulfide bonds. This solution was then diluted to the appropriate aptamer concentration in the respective buffer. The freshly cleaned electrodes were immersed into the appropriate concentration of aptamer for 1 h for probe immobilization. Following immobilization, the electrodes were rinsed with copious amounts of ultrapure water and then immersed in a 3 mM 6-mercapto-1-hexanol solution in water for 1 h to displace any nonspecifically adsorbed DNA and passivate the remaining electrode area.[19]

Electrochemical Interrogation

All electrochemical measurements were performed using a three-electrode cell (gold working electrode, platinum counter electrode and Ag/AgCl reference electrode) and a CH Instruments 630B potentiostat (CH Instruments, Austin, TX). Alternating current voltammograms were acquired in buffer using a 25 mV amplitude signal at 50 Hz (unless otherwise stated) over a potential window of −0.05 to −0.45 V versus Ag/AgCl (3 M NaCl).

The equilibration times of the two sensors were determined as follows. For the thrombin E-AB sensor, representative low and high probe density sensors were immersed in buffer solution containing 750 nM thrombin and ACVs were recorded every ~5–10 min for 3 h until a plateau in peak current was reached. In contrast differential pulse voltammetry (DPV) was employed to measure the equilibration time of the cocaine E-AB sensor due to its improved time resolution. This was performed using a potential window of −0.1 to −0.4 V, an amplitude of 0.1 V, a pulse width of 5 ms and a sample width of 2.5 ms. The interrogating electrode was immersed in stirred 1X SSC buffer solution followed by injection of cocaine to yield a final target concentration of 100 μM. The DPV scans were performed continuously throughout this process to monitor the sensor performance over the given time period.

In order to determine probe packing densities chronocoulometric experiments were acquired using 10 mM tris buffer (pH 7.4) or 0.5 mM RuHex in 10 mM tris buffer (pH 7.4). Electrodes were immersed in the respective solution for 10 min prior to the experiment. Two-step coulometry was performed stepping from 0 to −0.350 V to 0 V versus Ag/AgCl with a pulse period of 250 ms. The probe densities were calculated using a previously established method.[20] In brief, the measured charge acquired from the reduction of the RuHex that is electrostatically associated with the negatively charged backbone of the surface-bound aptamers is used to calculate the number of moles of phosphate (and thus number of probe DNAs) immobilized on the surface. Of note, we have previously measured probe densities using an AC voltammetric method;[15] we find here, however, that while this method reproducibly measures relative probe densities when the probe geometry is held fixed (e.g., all sensors employing the same aptamer structure),[3,21] probe-geometry-dependent changes in electron transfer efficiency preclude using this method to determine absolute probe densities (Figure 2). Thus the probe densities reported here are those determined using the chronocoulometric method.

Results

Here we have studied the optimization of two representative E-AB sensors – a signal-on sensor directed against the small molecule cocaine and a signal-off sensor directed against the protein thrombin (Figure 1). Each is comprised of a specific DNA aptamer (32 nucleotides for cocaine and 31 nucleotides for thrombin, see refs 6 and 3, respectively) that has been modified at its 5′-terminus with a thiohexyl group and at its 3′-terminus with a redox active methylene blue. E-AB sensors are fabricated by attaching these modified aptamers via self-assembly alkanethiol chemistry to 2 mm^2 gold electrodes.[18] Alternating current voltammetry (ACV) is then employed to monitor the two-electron, one-proton reduction of methylene blue, with the ACV peak current (current at $E = E°$) proportional to the number of methylene blue groups undergoing electron transfer.[22] In the absence of target the probe aptamers are thought to be partially (cocaine) or entirely (thrombin) unfolded.[3,23] Upon target binding the aptamer folds, which presumably fixes the position of the redox tag relative to the electrode surface, resulting in either an increase (cocaine) or decrease (thrombin) in electron transfer efficiency (Figure 1).

The relevant figure of merit for E-AB optimization is the signal gain (or suppression) observed at a given target concentration, which is the fractional increase (or decrease) in current observed

upon target binding. This is calculated by the relative change in peak signal upon addition of target from the original signal observed in the absence of target. Relative to absolute signaling current, signal gain also has the advantage of normalizing for differences in probe density (i.e., can be used to meaningfully compare sensors fabricated at different probe densities) and for any macroscopic changes in electrode area. We thus focus here on the effects of varying E-AB sensor fabrication and operational parameters on this measure.

Controlling the Packing of Aptamers on the Electrode Surface

The density with which probe aptamers are packed on the electrode surface is controlled by varying the concentration of thiolated oligonucleotide employed during sensor fabrication (Figure 2). Employing fabrication concentrations of 0.01–1.25 μM we reproducibly achieve probe densities ranging from 1.2×10^{11} to 4.4×10^{12} molecules/cm^2 and 5.7×10^{11} to 1.3×10^{13} molecules/cm^2 for the cocaine and thrombin E-AB sensors respectively (as defined using chronocoloumetry,[20,24]Figure 2). The maximum density achieved for the cocaine aptamer is reached at a fabrication concentration of ~0.3 μM, beyond which no further increases are observed (Figure 2B). This plateau presumably arises due to steric and electrostatic repulsion between the negatively charged aptamers. Consistent with this, the mean probe-to-probe separation obtained at the highest density, ~5 nm, approximates the expected radius of this aptamer, which is believed to be partially folded in the absence of target.[25] Packing of the thrombin aptamer also increases with increasing fabrication concentration, but plateaus at a mean probe-to-probe spacing of ~3 nm. The higher packing density achieved with this aptamer is consistent with previous studies suggesting that, in the absence of target, it adopts a random coil configuration,[26] allowing the it to pack more closely.

Effects of Probe Density on Signal Gain

E-AB sensor gain is a strong function of probe density (Figures 3 and 4). For example, while a high-density cocaine sensor exhibits only 60% gain, the gain increases dramatically as probe density falls and reaches ~200% at a coverage of 1.6×10^{12} molecules/cm^2 (we note that at still lower concentrations the observed faradaic current, and thus the signal/noise of our experiments, becomes poor and sensor gain is thus ill-defined; Figure 4, left). This represents a 6-fold increase relative to the gain of the initially described cocaine E-AB sensor[6] and renders this sensor among the highest gain of the more than half-dozen E-AB sensors reported to date.[3,5,6,8–10] Optimization of the packing density for the thrombin sensor likewise results in signal gain that varies over a ~3-fold range (Figure 4, right). For this sensor, however, optimal signaling (42% suppression) is observed at intermediate probe densities, with signaling decreasing at both lower and higher densities.

Effect of ACV Frequency on Signal Gain

The observation that E-AB gain is a function of probe density suggests that the collision dynamics of the redox tag may play a role in signaling.[15] This, in turn, suggests that E-AB signaling might be a sensitive function of the ACV frequency used to interrogate the sensor. To test this we have investigated the effects of changing ACV frequency on the signaling of cocaine and thrombin sensors fabricated at both low and high packing densities. We find, however, that E-AB signaling is relatively insensitive to AC frequency (Figure 5); while the gain of both sensors is essentially zero at very low frequencies, above 1 (cocaine) or ~50 Hz (thrombin) it rapidly plateaus at values that remain constant to at least 5000 Hz. Above this frequency the capacitive current is so great that it precludes measurement of the faradaic current.

Sensor Equilibrium Time

In addition to affecting signal gain, the molecular crowding associated with increasing probe density might also affect the rate with which sensors equilibrate.[15] Consistent with this, the equilibration time constant of the thrombin sensor doubles (from 11 to 20 min) as the density is increased 40-fold (Figure 6, right). It thus appears that the optimization of packing density sometimes represents a compromise between signal gain and equilibration time. The cocaine sensor, however, equilibrates more rapidly than the ~4 s required to record an electrochemical scan even at the highest densities we have investigated (Figure 6, left).

Effects of SAM Chemistry on Sensor Performance

The gain of the cocaine E-AB sensor improves with decreasing probe density up until the point at which the number of probe aptamers is so low that the signaling current becomes limiting (Figure 4). This, in turn, suggests that increasing the conductivity of the SAM, which would increase the signaling current, might support still lower probe densities and thus still higher gain. Thus motivated, we have characterized the properties of cocaine E-AB sensors fabricated using thinner, more conductive SAMs.[27,28] Specifically, we have characterized the performance of sensors fabricated using 2 and 3-carbon, hydroxyl-terminated thiols (C2, 2-mercaptoethanol and C3, 3-mercapto-1-propanol) in the hopes of observing increased electron transfer efficiency relative to the hydroxyl-terminated six-carbon passivating layers employed in the above-described studies. In doing so we find that, as expected, the absolute current increases with reduced SAM thickness. For example, whereas a sensor employing a C6 monolayer generates a peak current of 2.5×10^{-8} A, under the same conditions, sensors fabricated with C2 and C3 SAMs yield currents of 1.9×10^{-7} and 1.0×10^{-7} A, respectively (data not shown). Unfortunately, however, we find that the gain of the cocaine sensor *decreases significantly* with decreasing SAM thickness (Figure 7). For example, the gain of sensors fabricated using a three carbon SAM is ~80% of that observed for the six carbon SAM, that of two carbon SAMs is reduced by an order of magnitude.

Discussion

Here we report a systematic study of E-AB sensor optimization in terms of probe density, AC interrogation frequency and surface attachment chemistry. We find that the density with which the signaling aptamers are packed on the electrode surface strongly affects gain, with up to 6-fold improvements in signaling recorded (relative to the best previously reported value for the cocaine sensor).[6] In contrast, above rather low cutoffs the effects of AC frequency on the sensor response is relatively minor (Figure 5). Finally, we find that, despite exhibiting improved signaling current, sensors fabricated using short-chain SAMs exhibit significantly reduced gain.

Improved E-AB signaling can arise due to changes in electron transfer efficiency or changes in the folded-unfolded equilibrium of the surface bound aptamer. For example, the gain of a signal-on sensor will improve if electron transfer from the unfolded aptamer is reduced or if transfer from the folded aptamer is increased. Conversely, an increase in E-AB signaling (e.g., gain or suppression) will occur if the fraction of molecules unfolded in the absence of target is increased. The increased gain observed for the cocaine sensor at low packing densities, however, does not appear to be associated with this latter mechanism. If such was the case, the higher population of unfolded aptamers would, by shifting the equilibrium further toward the unfolded state, lower target affinity because binding would then have to overcome a more unfavorable folding free-energy, which is not observed (Figure 3).

The signaling of the cocaine sensor becomes poorer at higher probe densities. This may occur because, as the probes become more densely packed, some aptamers become inactive, reducing

the gain as fewer of the probes undergo binding-induced folding. This inactivation could result from unfavorable interactions between neighboring aptamers such as cross hybridization -a potential result of the self-complimentary nature of the individual aptamer sequences. Consistent with this, while the optimal packing density of the cocaine aptamer corresponds to mean probe-probe spacing that, at ~10 nm, is slightly greater than the 13 nm contour length expected for the fully unfolded aptamer,[29] this aptamer is thought likely to remain partially folded in the absence of cocaine[23] suggesting that 10 nm spacing would be sufficient to eliminate aptamer-aptamer interactions.

In contrast to the cocaine sensor, the signaling of the thrombin sensor is optimal at an intermediate probe density, corresponding to a mean probe-probe spacing of ~3.5 nm. This optimal spacing is similar to the 4.3 nm radius estimated for the aptamer-thrombin complex[30] and may arise as a consequence of two competing effects: while higher densities likely reduce thrombin affinity due to crowding, lower packing density may lead to increased mobility of the methylene blue tag and, in turn, increased electron transfer from the unfolded state.

We find that E-AB signaling is relatively insensitive to the ACV frequency employed to interrogate the sensor. Above the lowest AC frequencies we have investigated (1 Hz for cocaine and ~50 Hz for thrombin), we do not observe any significantly change in E-AB gain irrespective of the packing density of the sensor. This suggests that signaling may be limited by the intrinsic electron transfer rate from the methylene blue through the SAM. This limited ACV frequency dependence also reinforces the conclusion that the reduced gain observed at higher probe densities arises due to the inactivity of some aptamers under these conditions rather than via changes in the collision dynamics of the unfolded aptamer (which may be expected to change the AC frequency response of the sensor). This contrasts with the signaling mechanism of the closely related E-DNA sensor, which is clearly linked to binding-induced changes in collision dynamics.[15]

Finally, the performance of the cocaine E-AB sensor is strongly dependent on the nature of the SAM passivation layer, with thicker SAMs leading to reduced signaling current but increased gain (Figure 7). The increased gain is consistent with an increase in the fraction of aptamers unfolded in the absence of target (more aptamers unfolded leads to a greater change in current when all of the aptamers fold). Such an increase in the fraction of aptamers folded should, as described above, reduce the affinity of the aptamer for its target. Consistent with this, the dissociation constant observed for sensors fabricated with two-carbon SAMs is an order of magnitude lower than that observed for six carbon SAMs. While the ultimate origins of this effect are unclear, it may arise due to the longer "net" linker present in the 2-carbon construct. That is, because the aptamer sequence is linked to the surface via a 6-carbon chain in all three sensors (Figure 7), the DNA element is likely farther above the double layer that forms on the electrode.[31] Given that we are operating at a potential below the potential of zero charge on gold,[32] and aptamers within the double layer would experience a strong, negative electric field. This would, in turn, favor the extended, unfolded state. Similar electric field effects on the conformation of electrode-bound DNAs have previously been reported.[33] Alternatively, the thicker SAM (i.e., 6-carbon) may increase steric hindrance between the methylene blue and the SAM in the folded conformation of the aptamer. This could shift the equilibrium toward the unfolded state allowing for a greater change in current with the addition of target, albeit this should also reduce affinity for the target.

We have shown here that simple variations in E-AB fabrication significantly improve sensor performance. And while magnitude of these effects—and their optimal values—varies depending on the structure, the target and the sensing aptamer, the fabrication parameters described here serve as a basic outline for the optimization of new E-AB sensors in the future.

Acknowledgements

References

1. Willner I, Zayats M. Angew Chem Int Ed 2007;46:6408–6418.

2. Josep Lluis AS, Baldrich E, Radi A, Dondapati S, Sanchez PL, Katakis I, O'Sullivan CK. Electroanalysis 2006;18:1957–1962.

3. Xiao Y, Lubin AA, Heeger AJ, Plaxco KW. Angew Chem Int Ed 2005;44:5456–5459.

4. Xiao Y, Piorek BD, Plaxco KW, Heeger AJ. J Am Chem Soc 2005;127:17990–17991. [PubMed: 16366535]

5. Lai RY, Plaxco KW, Heeger AJ. Anal Chem 2007;79:229–233. [PubMed: 17194144]

6. Baker BR, Lai RY, Wood MS, Doctor EH, Heeger AJ, Plaxco KW. J Am Chem Soc 2006;128:3138–3139. [PubMed: 16522082]

7. Zayats M, Huang Y, Gill R, Ma CA, Willner I. J Am Chem Soc 2006;128:13666–13667. [PubMed: 17044676]

8. Zuo X, Song S, Zhang J, Pan D, Wang L, Fan C. J Am Chem Soc 2007;129:1042–1043. [PubMed: 17263380]

9. Ferapontova EE, Olsen EM, Gothelf KV. J Am Chem Soc 2008;130:4256–4258. [PubMed: 18324816]

10. Xiao Y, Rowe AA, Plaxco KW. J Am Chem Soc 2007;129:262–263. [PubMed: 17212391]

11. Radi AE, O'Sullivan CK. Chem Comm 2006:3432–3434. [PubMed: 16896485]

12. Hoa XD, Kirk AG, Tabrizian M. Biosens Bioelectron 2007;23:151–160. [PubMed: 17716889]

13. Fan C, Plaxco KW, Heeger AJ. Trends Biotechnol 2005;23:186–192. [PubMed: 15780710]

14. Warsinke A, Nagel B. Anal Lett 2006;39:2507–2556.

15. Ricci F, Lai RY, Heeger AJ, Plaxco KW, Sumner JJ. Langmuir 2007;23:6827–6834. [PubMed: 17488132]

16. Halperin A, Buhot A, Zhulina EB. Biophys J 2005;89:796–811. [PubMed: 15908581]

17. Yu F, Yao D, Knoll W. Nucleic Acids Res 2004;32:e75. [PubMed: 15155822]

18. Xiao Y, Lai RY, Plaxco KW. Nat Protocols 2007;2:2875–2880.

19. Herne TM, Tarlov MJ. J Am Chem Soc 1997;119:8916–8920.

20. Lao R, Song S, Wu H, Wang L, Zhang Z, He L, Fan C. Anal Chem 2005;77:6475–6480. [PubMed: 16194115]

21. Holden Thorp H. Trends Biotechnol 2003;21:522–524. [PubMed: 14624859]

22. O'Connor SD, Olsen GT, Creager SE. J Electroanal Chem 1999;466:197–202.

23. Stojanovic MN, de Prada P, Landry DW. J Am Chem Soc 2001;123:4928–4931. [PubMed: 11457319]

24. Steel AB, Herne TM, Tarlov MJ. Anal Chem 1998;70:4670–4677. [PubMed: 9844566]

25. Schultze P, Macaya RF, Feigon J. J Mol Biol 1994;235:1532–1547. [PubMed: 8107090]

26. Li JJ, Fang X, Tan W. Biochem Biophys Res Commun 2002;292:31–40. [PubMed: 11890667]

27. Smalley JF, Feldberg SW, Chidsey CED, Linford MR, Newton MD, Liu YP. J Phys Chem 1995;99:13141–13149.

28. Qi Y, Ratera I, Park JY, Ashby PD, Quek SY, Neaton JB, Salmeron M. Langmuir 2008;24:2219–2223. [PubMed: 18225934]

29. Meller A, Nivon L, Branton D. Phys ReV Lett 2001;86:3435. [PubMed: 11327989]

30. Reuter A, Dittmer WU, Simmel FC. Eur Phys J E 2007;22:33–40. [PubMed: 17334687]

31. Bard, AJ.; Faulkner, LR. Electrochemical Methods. Vol. 2nd. Wiley and Sons; New York: 2001.

32. Rentsch S, Siegenthaler H, Papastavrou G. Langmuir 2007;23:9083–9091. [PubMed: 17628087]

33. Kelley SO, Barton JK, Jackson NM, McPherson LD, Potter AB, Spain EM, Allen MJ, Hill MG. Langmuir 1998;14:6781–6784.
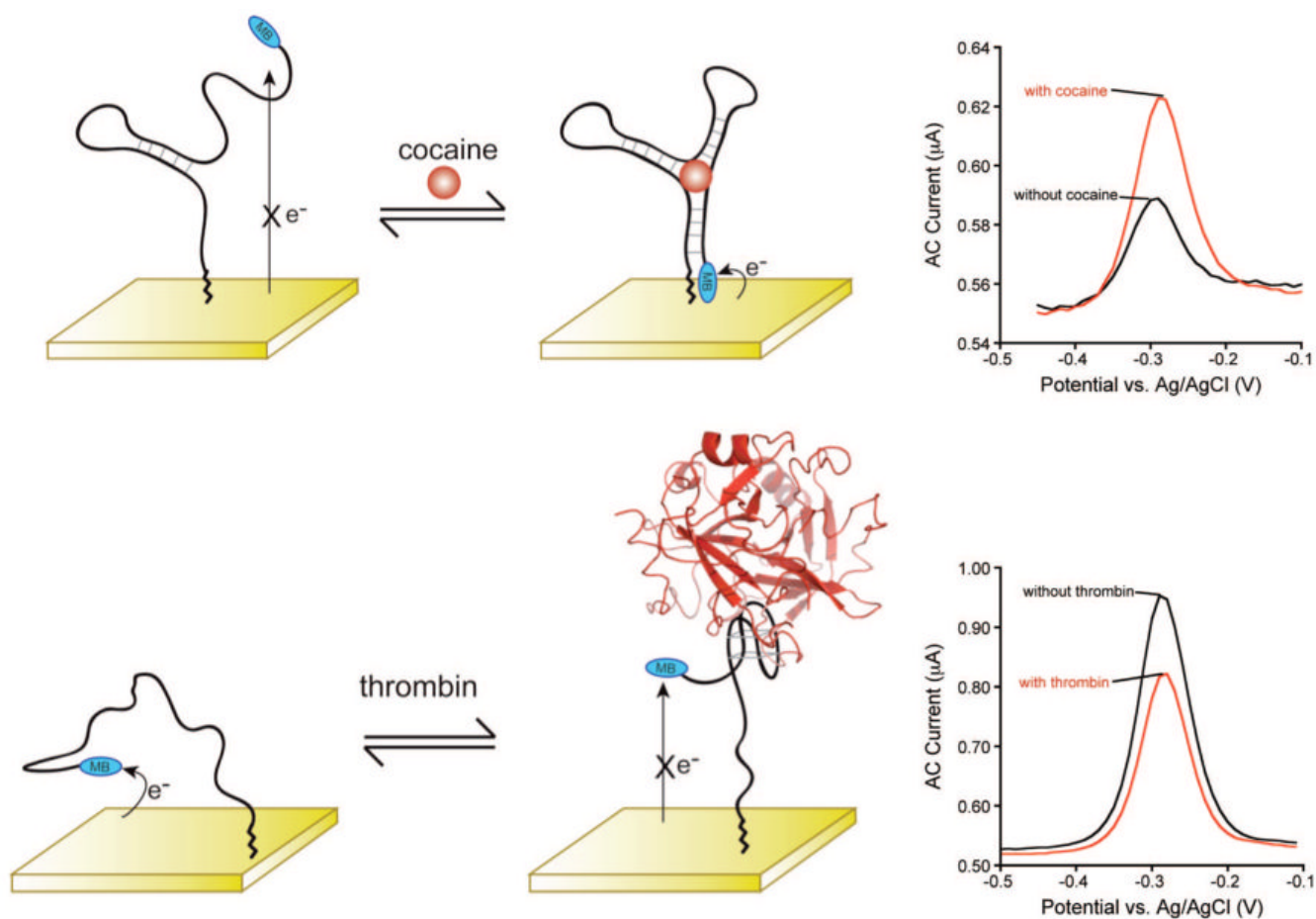
Figure 1.
E-AB sensors consist of a redox-tagged DNA or RNA aptamer directed against a specific target (left). In the absence of target, the aptamer remains relatively or entirely unfolded. Upon addition of target, the aptamer undergoes binding induced folding which brings the redox tag in proximity to the electrode, thus increasing faradaic current (e.g., cocaine E-AB sensor, top), or fixes the redox tag away from the electrode, reducing faradaic current (*e.g.*, thrombin E-AB sensor, bottom). (right) Alternating current voltammetry (AVC) is used to monitor the faradaic current arising from the tag and thus the presence of target.
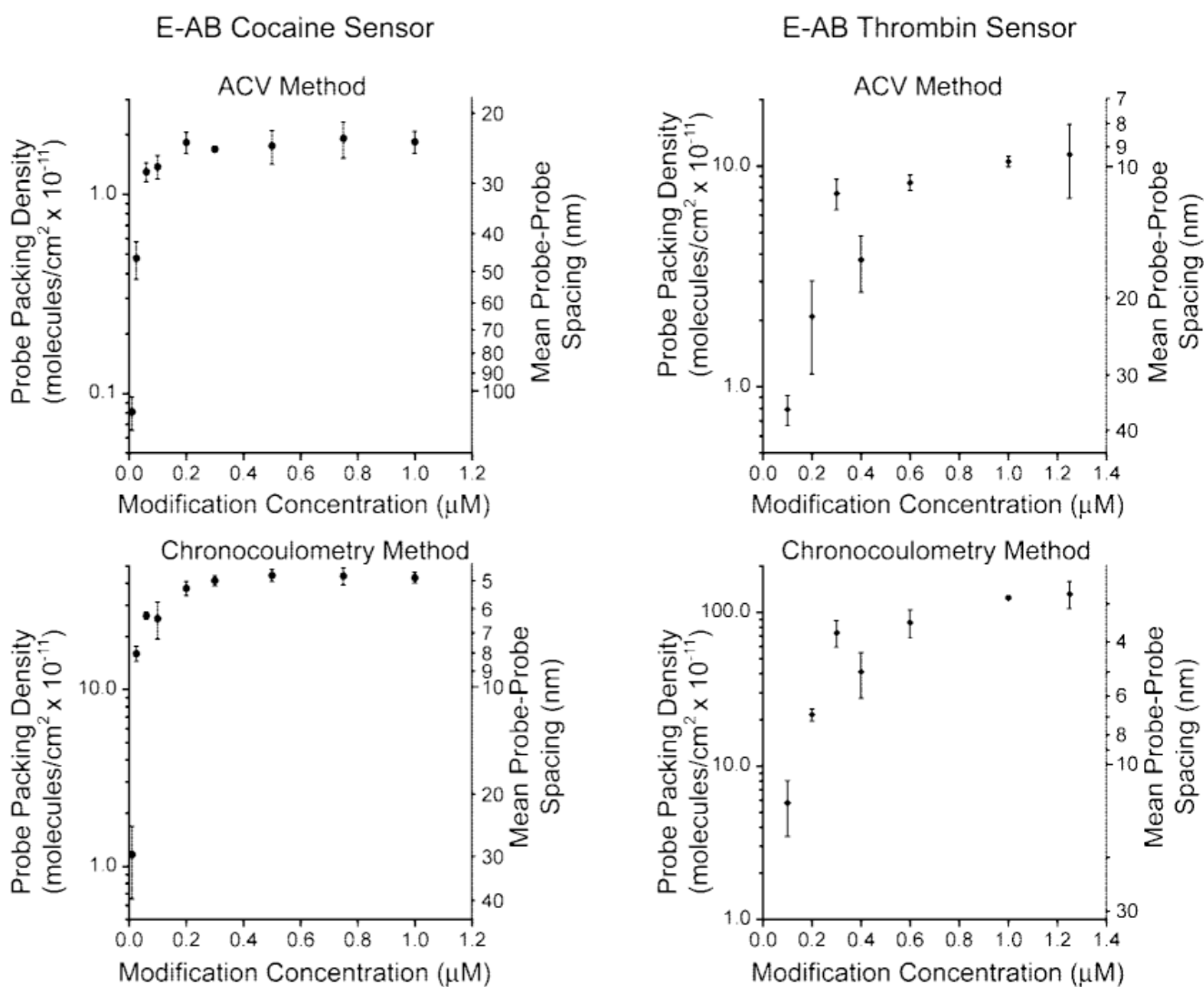
Figure 2.
Packing density of aptamers on the electrode surface is readily controlled by varying the concentration of probe DNA employed during sensor fabrication. As shown, ACV peak current (top) and chronocoulometry (bottom) methods produce correlated, but significant different estimates of probe density. We believe this occurs because the AC method is highly dependent on electron transfer efficiency, which in turn is dependent on probe geometry. We have thus reported chronocoulometric measurements throughout the body of this work. Values represent the average and standard deviations from three independent sensors at each probe density.
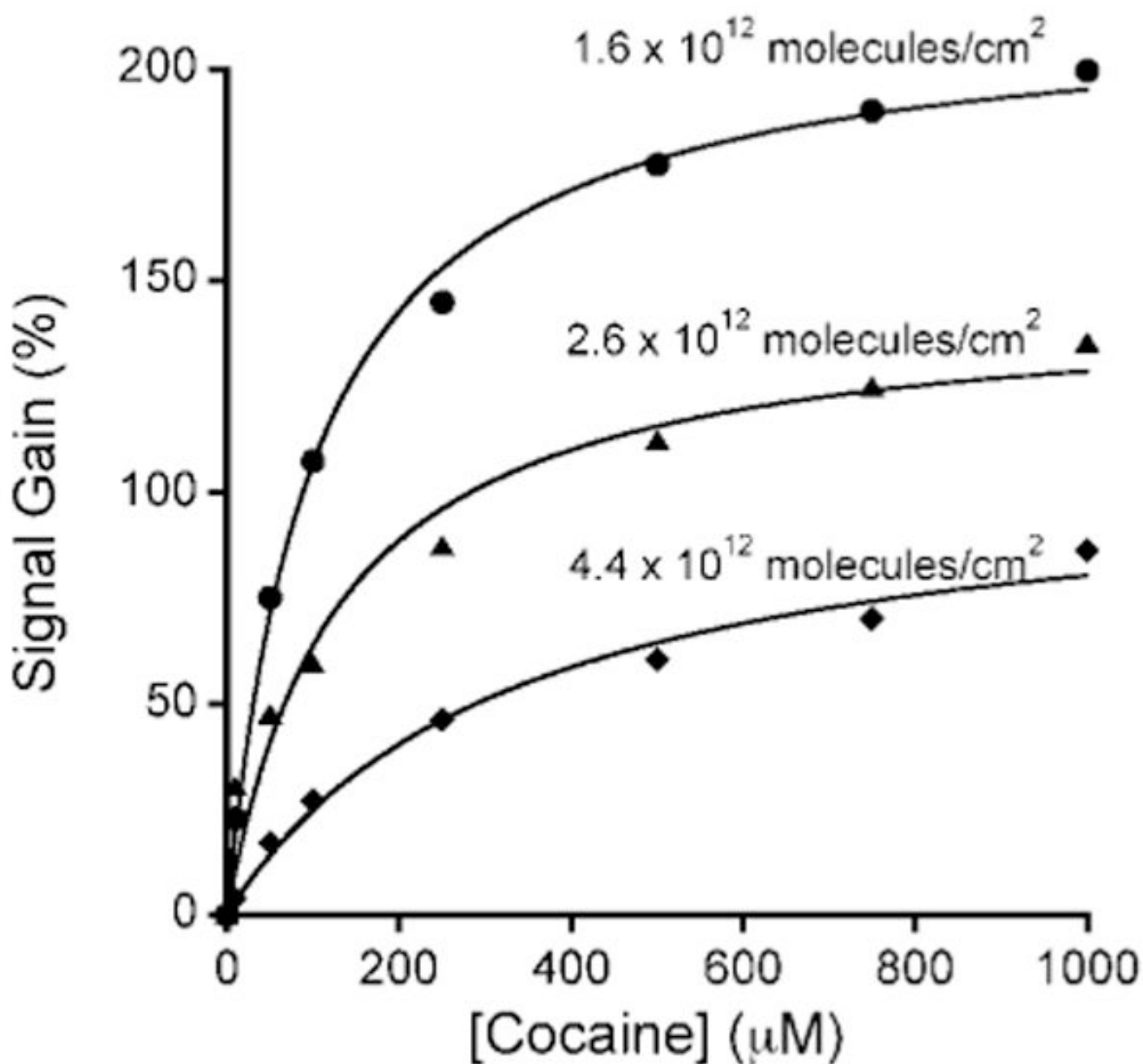
Figure 3.
Density with which probe aptamers are packed on the electrode strongly affects E-AB signal gain. For example, shown are the response curves of low medium and high-density cocaine sensors (fabricated using 25, 60, and 500 nM cocaine aptamer concentrations during fabrication). The solid lines represent hyperbolic binding curves with dissociation constants (K_d) of 327 ± 64, 101 ± 8 and 127 ± 35 μM respectively, which are comparable to the solution phase aptamer K_d of 100 μM.[23]
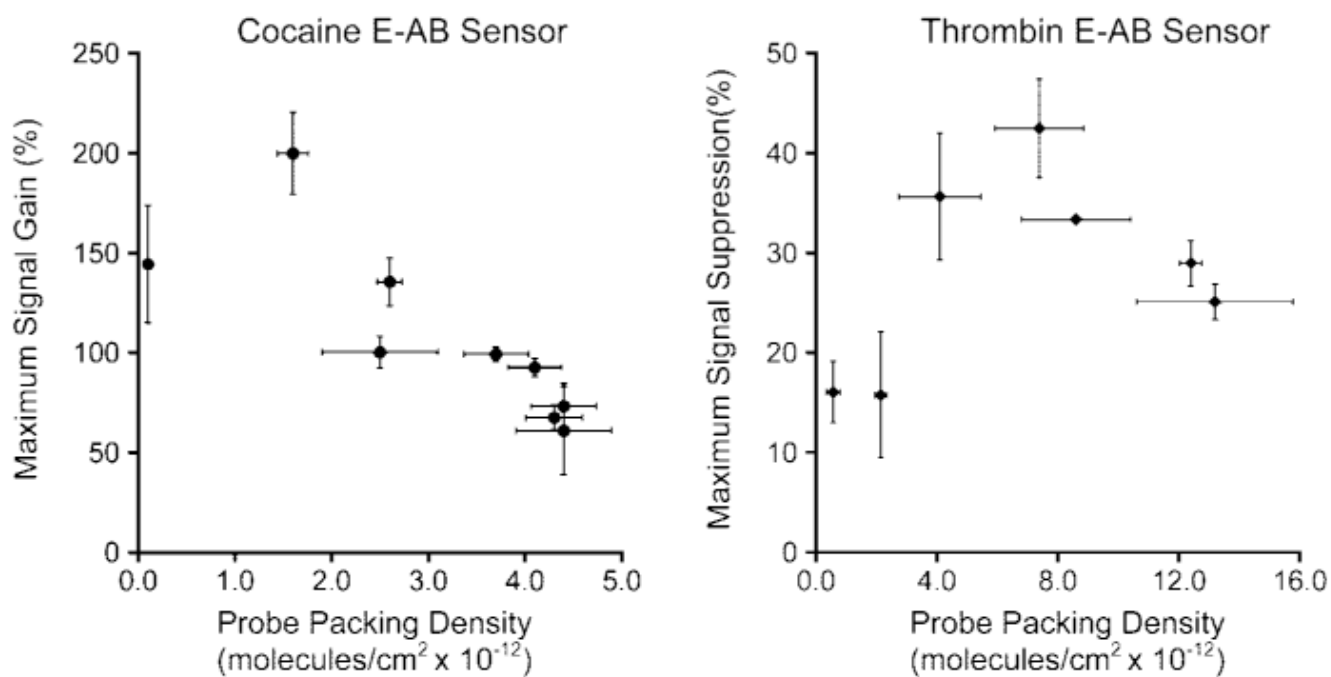
Figure 4.
Optimal probe density depends on the nature of the aptamer and its target. For example, while maximum gain is obtained for the cocaine sensor (left) at very low probe densities (the highest gain, 200%, is observed at a probe density of 1.6×10^{12} molecules/cm^2), optimal density for the thrombin sensor (right) is achieved at intermediate densities.
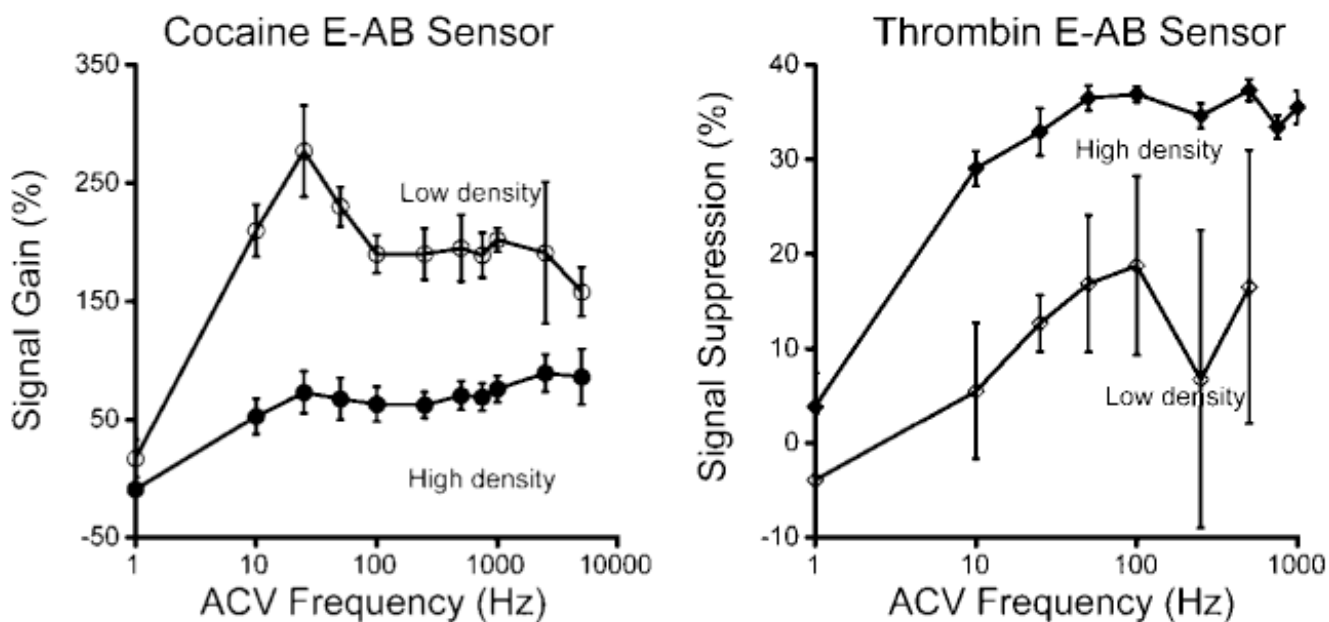
Figure 5.
At all but the very lowest frequencies, E-AB signaling is relatively unaffected by the ACV perturbation frequency used to interrogate the surface bound aptamers. This effect holds for both the cocaine (left) and thrombin (right) sensors and for both low (open circles) and high (filled circles) packing densities. Shown are data collected with low (1.6×10^{12} molecules/ cm^2) and high (4.3×10^{12} molecules/cm^2) density cocaine sensors and low (5.8×10^{11} molecules/cm^2) and high (1.3×10^{13} molecules/cm^2) density thrombin sensors.
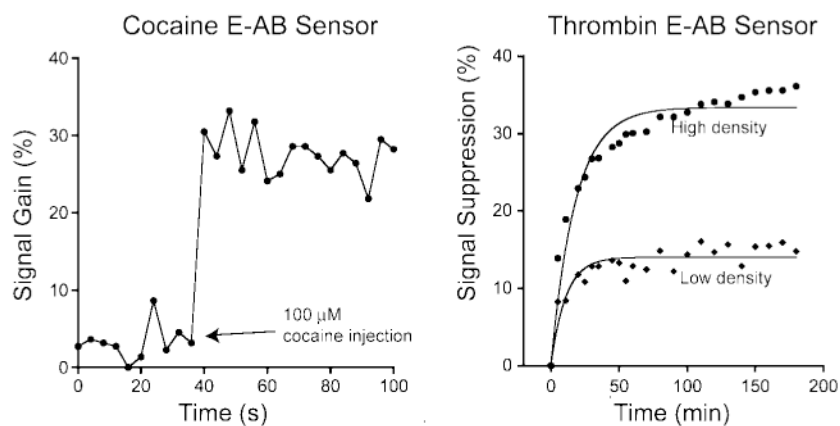
Figure 6.
Molecular crowding likely affects E-AB response times. We find, however, that the response time of the cocaine E-AB sensor (left) is extremely rapid: even high-density sensors (~4 × 10^{12} molecules/cm^2) equilibrate within the 4 s dead time of our electrochemical measurements. The thrombin sensor (right), in contrast, equilibrates much more slowly and exhibits the expected density dependence. The data points represent signal suppression measured after addition of 750 nM thrombin ($t = 0$). The solid lines represent a single-exponential fit to the data with rates of 0.05 and 0.09 s^{-1} for the high (1.3×10^{13} molecules/cm^2) and low (5.8×10^{11} molecules/cm^2) packing densities.
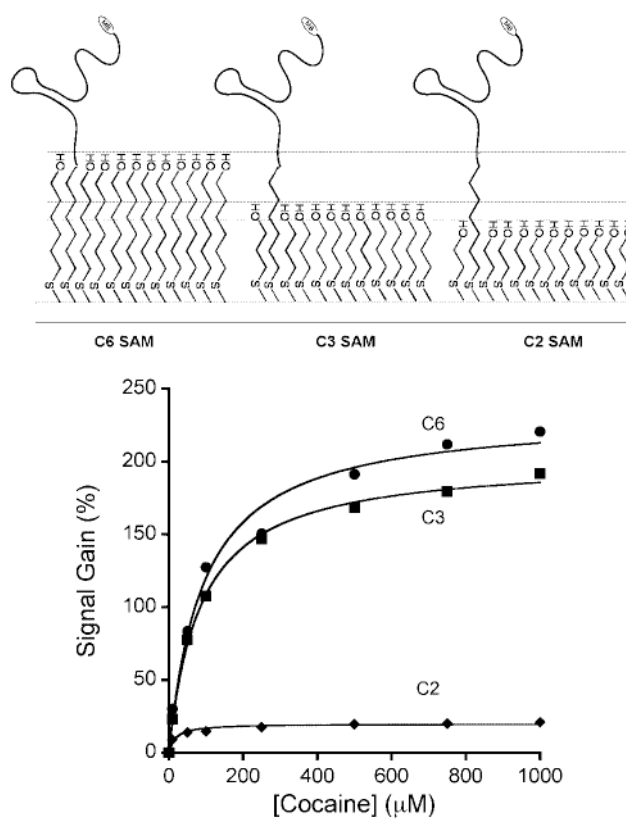
Figure 7.
Performance of the cocaine E-AB sensor is strongly affected by the thickness of the SAM layer used to passivate the electrode, with thicker SAMs leading to greater gain but lower affinity and poorer signaling current. Shown are binding curves for sensors fabricated using six-, three- and two-carbon alkane thiol SAMs (all at a probe density of 1.6×10^{12} molecules/cm^2). The solid lines represent a hyperbolic binding curve fit to the data with dissociation constants (K_d) of 95 ± 15, 86 ± 5, and $18 \pm 5 \mu$M for the six-, three- and two-carbon SAMs respectively.